



# Two-long terminal repeat (LTR) DNA circles are a substrate for HIV-1 integrase

Received for publication, November 30, 2018, and in revised form, April 8, 2019. Published, Papers in Press, April 10, 2019, DOI 10.1074/jbc.RA118.006755

Clémence Richetta<sup>†1</sup>, Sylvain Thierry<sup>†1</sup>, Eloise Thierry<sup>‡</sup>, Paul Lesbats<sup>§</sup>, Delphine Lapailierie<sup>§</sup>, Soundasse Munir<sup>‡</sup>, Frédéric Subra<sup>‡</sup>, Hervé Leh<sup>‡</sup>, Eric Deprez<sup>‡</sup>, Vincent Parissi<sup>§</sup>, and Olivier Delelis<sup>‡2</sup>

From the <sup>†</sup>Laboratoire de Biologie et Pharmacologie Appliquée, Centre National de la Recherche Scientifique UMR8113, ENS-Cachan, 94235 Cachan and the <sup>§</sup>Laboratoire de Microbiologie Fondamentale et Pathogénicité, Centre National de la Recherche Scientifique UMR5234, Université Victor Segalen Bordeaux 2, 33076 Bordeaux, France

Edited by Patrick Sung

Integration of the HIV-1 DNA into the host genome is essential for viral replication and is catalyzed by the retroviral integrase. To date, the only substrate described to be involved in this critical reaction is the linear viral DNA produced in reverse transcription. However, during HIV-1 infection, two-long terminal repeat DNA circles (2-LTRcs) are also generated through the ligation of the viral DNA ends by the host cell's nonhomologous DNA end-joining pathway. These DNAs contain all the genetic information required for viral replication, but their role in HIV-1's life cycle remains unknown. We previously showed that both linear and circular DNA fragments containing the 2-LTR palindrome junction can be efficiently cleaved *in vitro* by recombinant integrases, leading to the formation of linear 3'-processed-like DNA. In this report, using *in vitro* experiments with purified proteins and DNAs along with DNA endonuclease and *in vivo* integration assays, we show that this circularized genome can also be efficiently used as a substrate in HIV-1 integrase-mediated integration both *in vitro* and in eukaryotic cells. Notably, we demonstrate that the palindrome cleavage occurs via a two-step mechanism leading to a blunt-ended DNA product, followed by a classical 3'-processing reaction; this cleavage leads to integrase-dependent integration, highlighted by a 5-bp duplication of the host genome. Our results suggest that 2-LTRc may constitute a reserve supply of HIV-1 genomes for proviral integration.

Establishment of a stable infection by HIV-1 requires the insertion of the retroviral DNA into the host genome. This step is catalyzed by the viral integrase (IN)<sup>3</sup> using the linear viral DNA issued from the reverse transcription. HIV-1 IN catalyzes the 3'-processing of the viral U3 and U5 ends and then the integration of the newly 3'-processed ends into the target DNA

during a strand-transfer reaction (1–3). In addition to integrated DNA, several forms of unintegrated DNA can be detected in infected cells. Unintegrated viral genomes included a linear form generated from the reverse transcription process, circular forms resulting from autointegration, and circular genomes harboring one- or two-long terminal repeats (LTRs) (1-LTR circles, 1-LTRc; and 2-LTR circles, 2-LTRc, respectively) (4). If no integration occurs, linear viral DNA is rapidly degraded or circularized into 1- or 2-LTRc (4–7). 2-LTRc are generated by ligation of the cDNA ends by the host cell nonhomologous end-joining (NHEJ) pathway (8). Additionally recombination between the 2-LTRs of linear DNA can lead to 1-LTR DNA circles (1-LTRc). These circular genomes are detected in the nucleus of infected cells, even if a portion of 1-LTRc originates from reverse transcription (4). Previous studies have shown that, by inhibiting the integration process with strand-transfer inhibitors such as Raltegravir (RAL), the amount of 2-LTRc substantially increases both in cell cultures and in patients (9, 10). To date, the role of the 2-LTRc remains misunderstood. They are usually described as by-products of the reverse transcription, without any significant role in the HIV-1 replication. However, they could be involved, with 1-LTRc, in a weak transcription of HIV-1 accessory genes, such as *Nef* (11), proving their potential role during infection. Recently, it has been reported that viral production could be detected from unintegrated DNA forms following infection of resting CD4 T cells, supporting their role in the overall replication process (12, 13).

Interestingly, the HIV-1 2-LTR junction, formed by the ligation of the LTR extremities in infected cells is palindromic. Furthermore, several studies have shown that both oligonucleotides and circular DNA, containing the palindromic junctions, can be cleaved *in vitro* by recombinant HIV-1 and primate foaming virus-1 INs, leading to the formation of linear 3'-processed-like DNA (14–16). Consistently, our recent study highlighted that unintegrated viral DNA, more particularly 2-LTRc, could be used as a reserve supply of genomes for proviral integration (15). These results suggest that the 2-LTRc could serve as functional intermediates in the retrovirus replication cycle, which implies that IN can cleave the palindromic junction of the 2-LTRc, leading to linear DNA that can be subsequently integrated into the target DNA. This hypothesis was addressed in the present work both at the biochemical level and in a

This work was supported by French National Research Agency against AIDS (ANRS) Grant EOTP 342901 (to O. D.) and the Centre National de la Recherche Scientifique. The authors declare that they have no conflicts of interest with the contents of this article.

<sup>1</sup> Both authors contributed equally to this manuscript.

<sup>2</sup> To whom correspondence should be addressed. Tel.: 33-0-1-47-40-59-74; Fax: 33-0-47-40-76-71; E-mail: delelis@lbpa.ens-cachan.fr.

<sup>3</sup> The abbreviations used are: IN, integrase; LTR, long terminal repeat; RAL, Raltegravir; ODN, oligonucleotide; HSI, half-site integration; FSI, full-site integration; LM-PCR, ligation-mediated PCR; LTRc, long terminal repeat circle; eGFP, enhanced green fluorescent protein; CMV, cytomegalovirus; LEDGF, lens epithelial-derived growth factor.

eukaryote cellular context. We particularly addressed the question of whether the viral DNA ends formed upon 2-LTR junction cleavage could be compatible with strand-transfer and full-integration reactions and, whether the integration reaction occurs via an IN-dependent mechanism, *i.e.* leading to the 5-bp duplication of the host genome.

Biochemical analyses led us to show that HIV-1 IN catalyzes the formation of integrated products from the LTR-LTR junction oligonucleotides using *in vitro* concerted integration assay. The physiological relevance of this process was further addressed in the previously established yeast integration eukaryotic model (17) as well as in the virological context, showing that IN also catalyzes the integration of a DNA substrate containing the 2-LTRc junction into genomic DNA. Our data highly suggest that 2-LTRc can serve as substrates for HIV-1 IN and, thus, may serve as a new source for the retroviral genome integration. This leads us to reconsider the different ways for the HIV-1 integration and, also, to re-analyze the impact of the 2-LTRc accumulation particularly during anti-IN treatments.

## Results and discussion

### *In vitro* cleavage of the 2-LTR palindromic junction by IN is improved by LEDGF/p75 and inhibited by RAL

An oligonucleotide (ODN) mimicking the palindromic sequence found at the LTR-LTR junction was previously shown to be efficiently cleaved by HIV-1 IN *in vitro*, leading to the formation of viral ends required for integration (13). Moreover, the cellular IN cofactor LEDGF/p75 has been involved in the enhancement of IN activity (18). Therefore, we have first analyzed whether LEDGF/p75 could also promote this cleavage. Using the 38-bp DNA mimicking the 2-LTR junction (referred as U5·U3, Fig. 1A, left) in the palindrome cleavage assay, we showed that LEDGF/p75 increased cleavage efficiency mediated by IN by a 3-fold factor (Fig. 1B). The resulting product of IN-mediated cleavage is 5'-TGTGGAAATCTCTAGCA, indicated as 5'-AGCA on the left of the gel.

Then, to better mimic a two-LTR circle, the 2-LTR junction fragment was inserted in a plasmid containing a constitutive yeast TEF1 promoter-dependent Zeocin resistance gene (named U5·U3 circle, Fig. 1A, right) and used as substrate for HIV-1 IN cleavage (Fig. 1C, upper panel). Incubation of the U5·U3 circle substrate with IN led to a protein concentration-dependent linearization of this DNA with an optimal activity reached at 1  $\mu$ M IN (Fig. 1C, upper panel). In this condition, 50% of the plasmid was linearized (indicated *L* in Fig. 1C, corresponding to the signal obtained by linearization of U5·U3 circle with SalI (lane 4)). The specificity of the cleavage was assessed using the catalytically inactivated D116A IN as well as the plasmid deleted of the palindromic junction (replaced by a random sequence: random circle, Fig. 1C, right panel). In these conditions, less than 5% of the plasmid DNA was linearized (Fig. 1C, right panel), highlighting a very poor contaminating nonspecific endonuclease activity in IN preparations. Taken together, these data indicate that the linearization of the DNA substrate by the WT IN was due to specific IN catalytical properties and was dependent of the presence of the palindromic junction.

Moreover, incubation of U5·U3 circle substrate with IN in the presence of LEDGF showed that this IN cofactor can increase the palindrome cleavage efficiency not only when located on a short DNA sequence as mentioned above, but also of a circular substrate (Fig. 1D, left). The cleavage quality was then checked by sequencing the viral ends resulting from incubation of the U5·U3 circle with IN or IN-LEDGF, as previously described by Munir and colleagues (4). A main proportion of the correct 3'-processed ends (AGCA) was found after the cleavage reaction by HIV-1 IN, as reported in Fig. 1D, right panel. Interestingly, a higher proportion of blunt ends (AGCAGT) was observed in the presence of LEDGF. This confirmed that the retroviral enzyme can generate canonical processed viral ends starting from the LTR-LTR junction, compatible with the strand-transfer reaction, but it also indicates that interaction of IN with LEDGF can generate viral DNA ends compatible with the 3'-processing reaction.

To better assess the specificity of the cleavage, we next analyzed the inhibition of the 2-LTR junction cleavage by IN using RAL treatment. Results shown in Fig. 2A revealed that cleavage of the DNA (38 bp) containing the palindromic sequence, in the presence or absence of LEDGF/p75, is inhibited by RAL in a dose-dependent manner. Similarly, RAL efficiently inhibited cleavage of the U5·U3 circle in a dose-dependent manner independently of the presence of LEDGF (Fig. 2B). Remarkably, the IC<sub>50</sub> found for the inhibition of the palindrome cleavage (500 to 900 nM) is closer to the IC<sub>50</sub> found for the inhibition of the 3'-processing reaction (micromolar range) (19) than the IC<sub>50</sub> characterizing the strand-transfer reaction (around 5 nM) (19), suggesting that endonucleolytic cleavage of the palindromic junction requires a DNA/IN complex more comparable with the one involved in 3'-processing than to the one involved in the strand-transfer reaction.

### *In vitro* integration of the U5·U3 junction directs reaction toward full-site integration

To determine whether this cleaved 2-LTR DNA can be further involved as an integration substrate, concerted integration assays were performed with the U5·U3 substrate. Integration efficiency was then compared with the one obtained with the DNA (38 bp) mimicking the viral DNA end found in infected cells (U5) (Fig. 3A). Integration products were detected after incubation of the U5·U3 DNA, pBSK acceptor vector, and IN under standard conditions previously established (20). The formation of all the expected half-site (HSI) and full-site integration (FSI) products were catalyzed by IN (Fig. 3A). Comparison of the integration profiles obtained with U5·U3 or U5 substrates indicates substantial variation in terms of enzyme concentration optimum. Indeed, the maximum integration efficiency using the U5·U3 or U5 DNA was obtained with 1  $\mu$ M and 500 nM IN, respectively (Fig. 3A, right). This difference is in accordance with the one previously described in cleavage assays (13) and suggests that different IN oligomers or structures are involved in the integration depending on the U5·U3 or U5 substrates. Furthermore, no integration product was obtained using a random DNA (Random), indicating that the integration reaction strictly requires the presence of the viral sequences (Fig. 3A, right).

## Integrase and 2-LTR circles

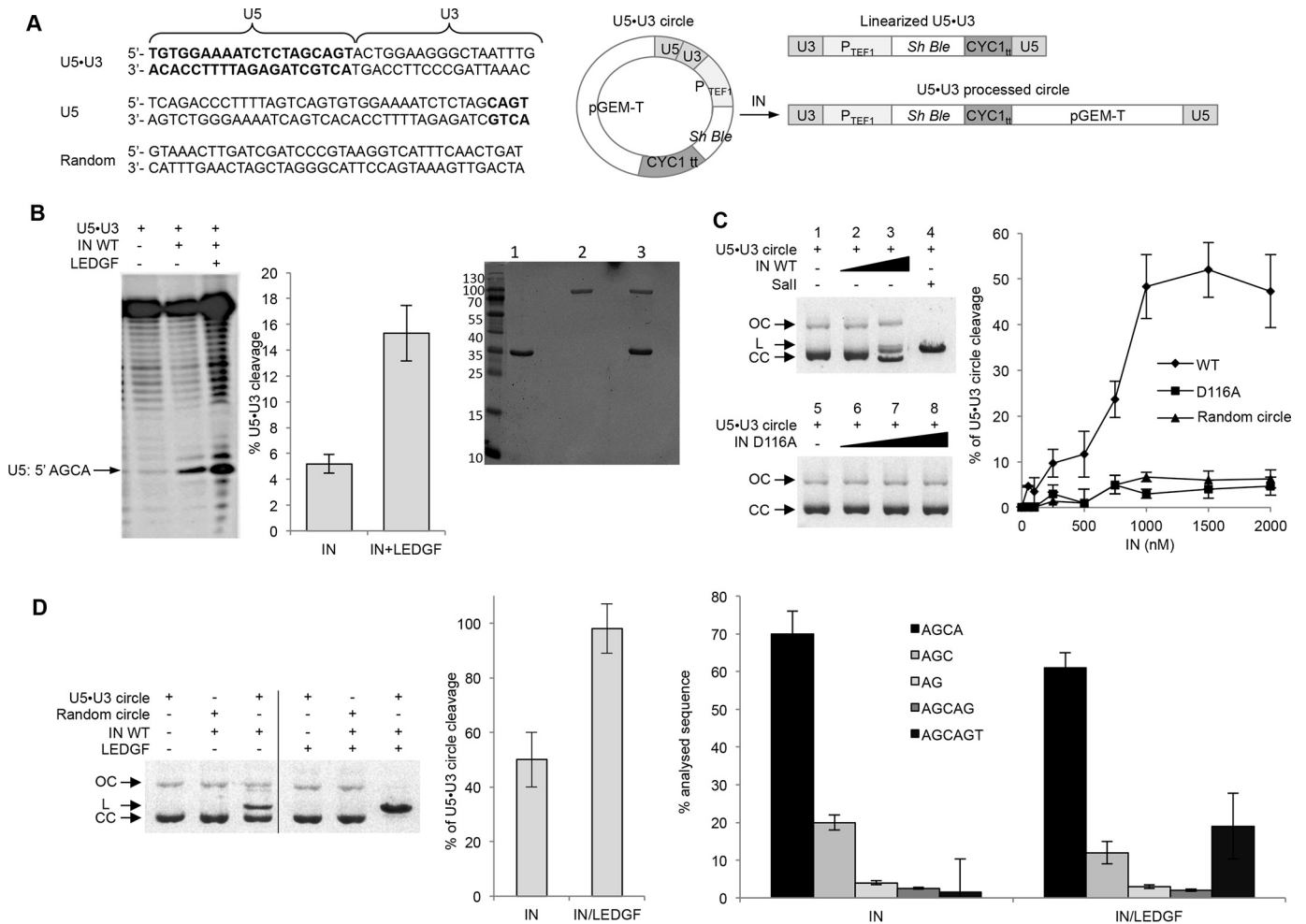


**Figure 1. IN-mediated cleavage of linear or circular DNA substrates containing the 2-LTR junction is improved by LEDGF.** *A*, linear and circular DNA substrates. The dsDNA (38 bp) mimicking the palindromic junction (U5-U3), the HIV-1 U5 end (U5), or carrying a nonviral random sequence (Random) were used in *in vitro* cleavage assays. The U5-U3 DNA was formed by hybridization of U5 5'-TGTGGAAAATCTCTAGCAGTACTGGAAGGGCTAATTTG and U3 5'-CAAATTA-GCCCTTCCAGTACTGCTAGAGATTTCCACA ODN. For the U5-U3 DNA, the U5 sequence (in *bold*) and the U3 sequence are indicated. For the U5 DNA, the CAGT end of the U5 end is indicated in *bold*. The unprocessed 1200-bp linear yeast integration substrate (linearized U5-U3) containing the two viral U3 and U5 ends was obtained by PCR amplification of the P<sub>TEF1</sub>ShBleCYC1<sub>tt</sub> fragment from the pTEF1/Zeo plasmid (Invitrogen) as described in Ref. 17. The 4237-bp two HIV-1 LTR junction circle (U5-U3 circle) was generated by pGEM-T cloning of the DNA fragment 2LTRP<sub>TEF1</sub>ShBleCYC1<sub>tt</sub> obtained by PCR amplification of the P<sub>TEF1</sub>ShBleCYC1<sub>tt</sub> cassette from the pTEF1/Zeo plasmid (Invitrogen) using 3'-Cont-Zeo (5'-TTGCAAATTAAGCCTTCGAGCGTCCC-3') and 5'-2LTR junction-Zeo (5'-TGTGGAAAATCTCTAGCAGTACTGGAAGGGCTAATTTGCCACACACCATAGCTTCAAATGTTTCTACTCC-3') primers. The 4237 processed 2-LTR junction (U5-U3 processed circle) was generated by IN-mediated cleavage as described in *C. P. TEF1*, yeast TEF1 promoter; *Sh Ble*, Zeocin resistance encoding gene. *B*, *left panel*: 1 μM IN ± 3 μM LEDGF were incubated for 1 h at 37 °C with 10 nM U5-U3 DNA (38 bp). In this experiment U5 ODN was radiolabeled at the 5' end. Reaction products were loaded on an 18% acrylamide gel. Products were quantified using the ImageJ software and the percentage of cleavage was reported (*middle panel*). The *arrow* shows the location of the cleavage mediated by IN on the radiolabeled U5 ODN. The resulting cleavage product is 5'-TGTGGAAAATCTCT-AGCA indicated as 5': -AGCA on the *left* of the denaturing gel. *Right panel*: Coomassie-stained gel image of the purified protein. *Lane 1*, integrase (IN). *Lane 2*, LEDGF/p75. *Lane 3*, IN/LEDGF complex. The molecular weight of the protein ladder is indicated in kilodaltons (PageRuler, Thermo Fisher). *C*, cleavage assay of the U5-U3 circle (300 ng) performed in the presence of increasing concentrations of WT (*lanes 2* (500 nM) and 3 (1 μM)) or inactivated D116A IN (*lanes 6* (500 nM), 7 (750 nM), and 8 (1 μM)). *Lane 4*, positive control, U5-U3 linearized by Sall digestion. Control experiment was performed using the Random circle obtained by cloning the random sequence (38 bp) into the pGEM-T vector, with increasing concentrations of WT IN (*right panel*). The positions of the close circular native (CC), open circular single strand cut (OC), and linearized double strand cut (L) plasmid DNA are reported. The percentage of linearized substrate was quantified by densitometry estimation using ImageJ software and reported (*right panel*). All the values correspond to the mean ± S.D. (*error bars*) of three independent sets of experiments. *D*, the same assay was performed with or without LEDGF (3 μM), IN WT (500 nM), and U5-U3 circle (300 ng), or Random circle (300 ng) substrate. The percentage of linearized substrate was quantified as mentioned above and reported (*middle panel*). Sequences of the linearized products were obtained as previously described under "Experimental procedures."

We further analyzed the quality of the integration products obtained, by comparing the integration profiles observed with U5-U3 or U5 DNA using optimal IN concentration for both substrates, *i.e.* 1 μM and 500 nM, respectively. As reported in Fig. 3B, the proportion of FSI *versus* HSI products obtained with either the U5-U3 or the U5 DNA was different. Indeed, using the one viral U5 ended DNA led to a major proportion of HSI integration (80% of integration products), whereas only a small

proportion of FSI integration was observed (20% of integration products). In contrast, when the U5-U3 was used as substrate for concerted integration, the proportion of FSI was clearly improved (50% of integration products), indicating that the pre-cleavage of the 2-LTR junction by IN could drive the reaction toward a FSI reaction with higher efficiency than when using the U5 end DNA (Fig. 3B, *right panel*). The reaction specificity was checked using RAL that specifically inhibits the

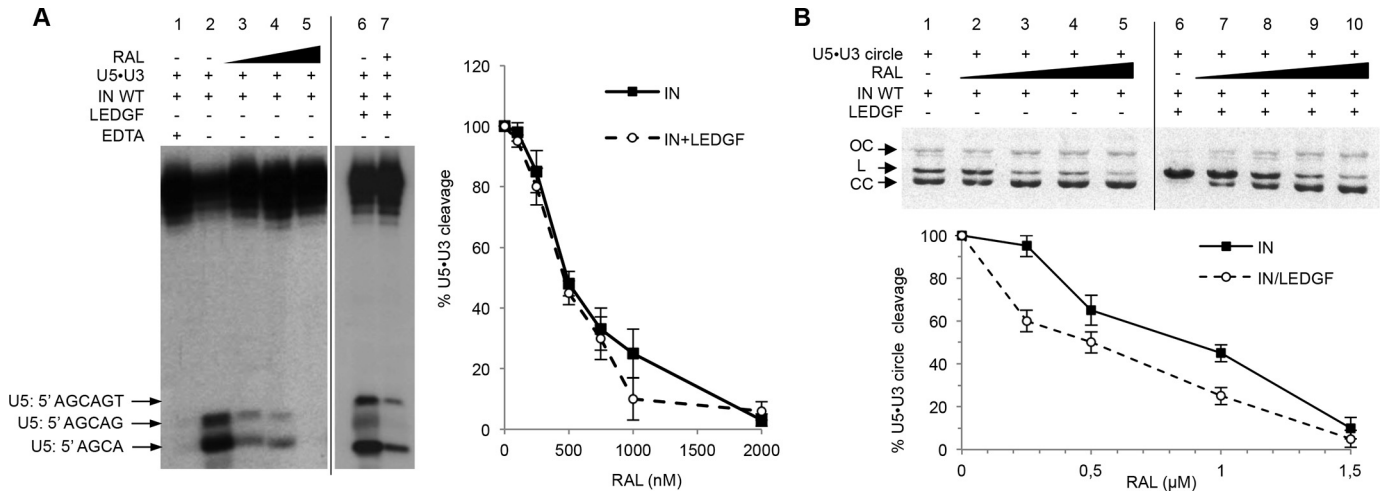


**Figure 2. IN-mediated cleavage of U5-U3 junction is inhibited by RAL.** *A*, left panel, cleavage of the palindrome was performed using 12 nM U5-U3 DNA in the presence of 1  $\mu$ M IN and 500 nM EDTA (1), 0 nM (2), 500 nM (3), 1000 nM (4), or 1500 nM (5) RAL. The same experiment was performed using 1  $\mu$ M IN and 3  $\mu$ M LEDGF in the absence (6) or presence (7) of 500 nM RAL. The products of the reaction were quantified using ImageJ software and reported as a percentage of cleavage from the substrate, right panel. *B*, 2-LTR junction cleavage assay was performed with the U5-U3 circle substrate (300 ng), in the presence of 500 nM IN and 0 (1), 50 (2), 100 (3), 250 (4), or 500 (5) nM RAL. The same experiment was performed in the presence of 3  $\mu$ M LEDGF (6–10) using 0 (7), 500 (8), 1000 (9), or 1500 nM (10) RAL. The gel from one representative experiment is shown. The cleavage products from three independent experiments were quantified as described above and the percentage of linearized substrate for IN alone or in the presence of LEDGF with increasing concentration of RAL, was reported below the gels.

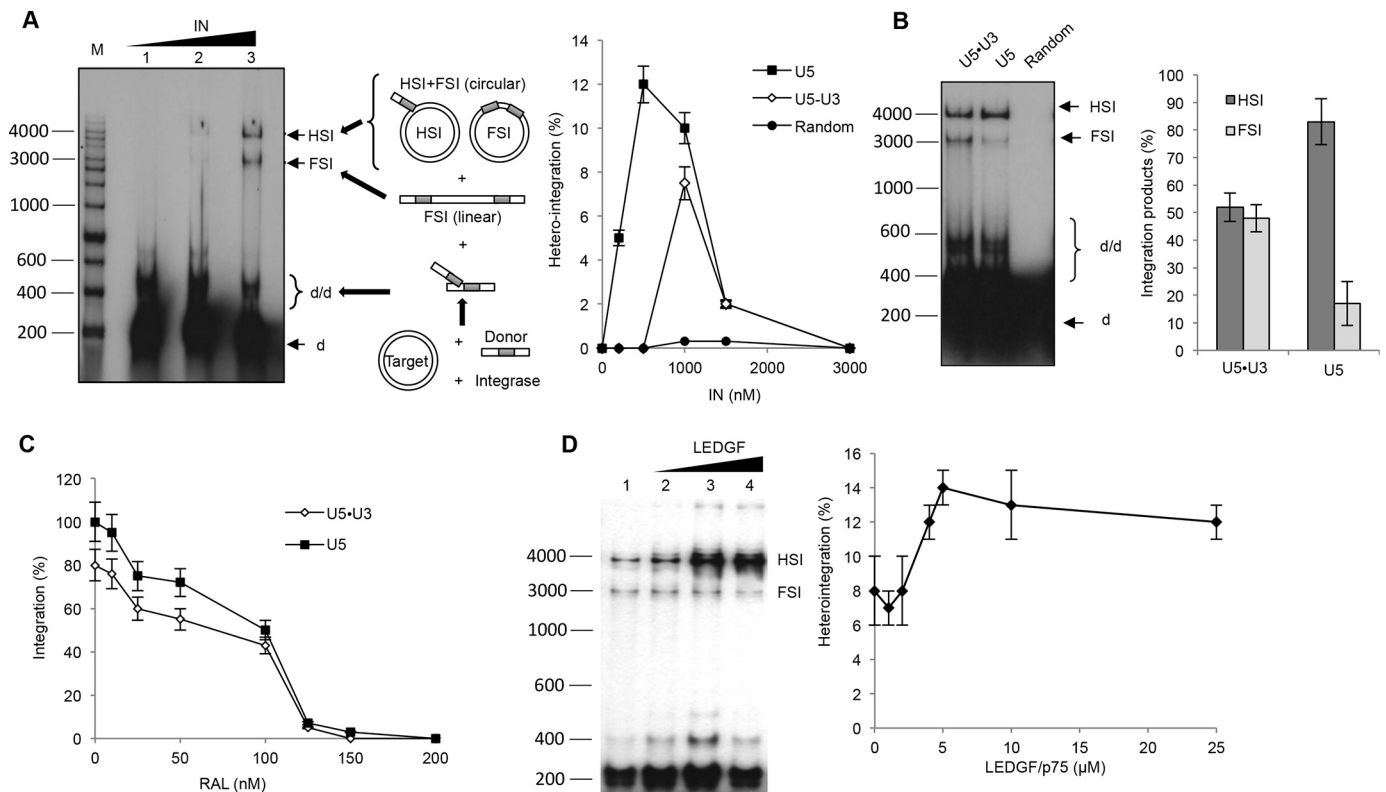


**Figure 3. Concerted integration by IN of a substrate containing the 2-LTR junction.** *A*, concerted integration assay was performed with 100 ng of pBSK-zeo acceptor plasmid, 10 ng of the 5'- $^{32}$ P-labeled U5-U3 donor DNA, and 0.25 (1), 0.50 (2), or 1.00 (3)  $\mu$ M IN. The reaction products were loaded on a 1% agarose gel. The position and structures of the donor substrate and different products obtained after HSI, FSI, and donor/donor integration (d/d) are explicitly shown. The heterointegration products (FSI + HSI) were quantified by densitometry estimation using ImageJ software and reported (right panel). *B*, integration reactions were performed using 1  $\mu$ M IN, 100 ng of pBSK-zeo acceptor plasmid, and 10 ng of the 38 bp of 5'- $^{32}$ P-labeled 2-LTR junction (U5-U3), the viral end U5 fragment, or Random donor DNA. The different integration products obtained were quantified by densitometry estimation using the ImageJ software. The proportion of FSI and HSI was evaluated for each integration condition and reported in the right panel. *C*, the concerted integration assay was performed in the same conditions as described in *A*, in the presence of increasing RAL concentrations. The heterointegration products (FSI + HSI) detected on the agarose gel were quantified by densitometry estimation using ImageJ software. *D*, concerted integration assay was performed with 1  $\mu$ M IN, 100 ng of pBSK-zeo acceptor plasmid, 10 ng of the 38 bp 5'- $^{32}$ P-labeled U5-U3 DNA, and in the presence of increasing LEDGF concentrations (0 (1), 2.5 (2), 5 (3), or 10  $\mu$ M (4)). The heterointegration products (FSI + HSI) obtained under these conditions and detected on agarose gel were quantified by densitometry estimation using ImageJ software and reported in the right panel. All values obtained from the described experiments correspond to the mean  $\pm$  S.D. (error bars) of at least three independent sets of experiments.

## Integrase and 2-LTR circles

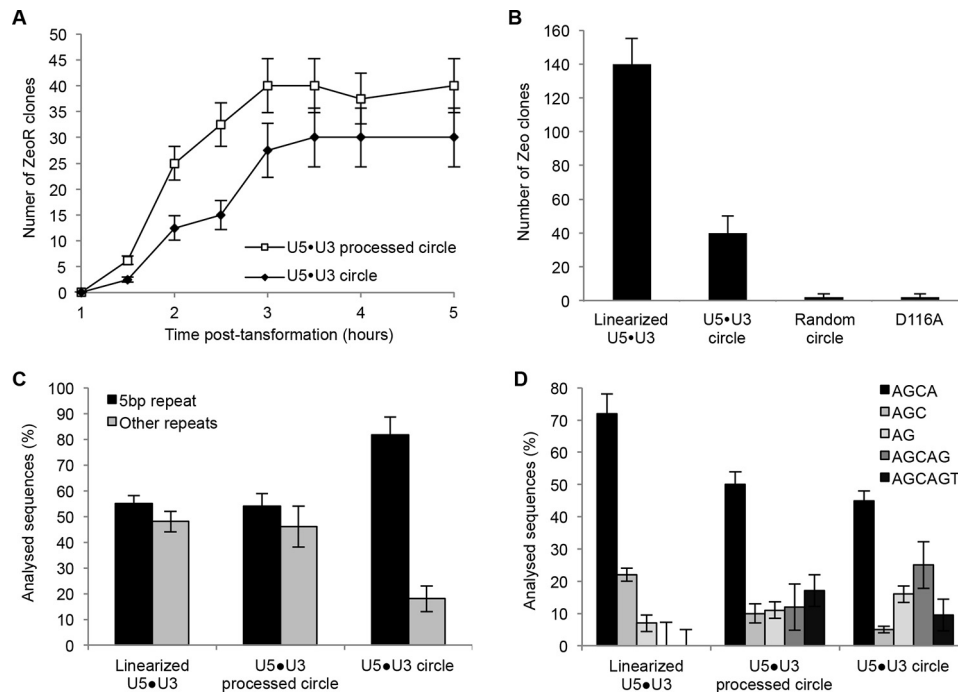


**Figure 4. Integration of 2-LTR junction DNA into yeast chromosome.** Yeast integration assay was performed as described in Ref. 17 and under “Experimental procedures” using either the 2-LTR junction circle or the processed 2-LTR junction obtained and purified as indicated in the legend of Fig. 1C. *A*, number of Zeocin-resistant clones selected after 1–5 h post-transformation with U5•U3 circle or U5•U3 processed circle. *B*, same experiments performed with the U5•U3, U5•U3 circle, or Random circle substrates after expression of the WT IN, or with the U5•U3 circle after expression of the inactivated D116A enzyme. *C* and *D*, 100 clones obtained in the yeast integration assays performed using the linear U5•U3, processed U5•U3 circle, or U5•U3 circle were sequenced as reported under “Experimental procedures.” *C*, number of correct 5-bp duplications and other repeats found at each extremities of the integrated DNA. *D*, the viral end sequence was also analyzed by sequencing and the number of clones harboring the correct AGCA viral ends or other structures is reported.

gration reaction (21). As reported in Fig. 3C, RAL induced a strong inhibition of the integration in a dose-dependent manner from both U5•U3 and U5 DNA indicating that the reaction was catalyzed by IN with a strand-transfer intermediary mechanism similar to the typical integration of the linear viral sequence ended substrate. Taken together, our data demonstrate that a DNA mimicking the palindrome found at the HIV-1 2-LTR junction can serve as integration substrate *in vitro*.

Previous analyses of the palindrome cleavage by HIV-1 IN led us to demonstrate that the reaction was optimally performed by tetrameric enzyme (13). The IN tetramerization on the palindromic junction could improve the further concerted integration step because this oligomeric state has been shown to be involved in this specific activity (22–25). Because the cellular IN cofactor LEDGF/p75 has been previously shown to stabilize IN tetramers (18), we performed concerted integration assays using the U5•U3 DNA substrate to study the influence of LEDGF/p75 on integration efficiency. As reported in Fig. 3D, LEDGF/p75 stimulates in a dose-dependent manner the integration reaction using the U5•U3 substrate, and more particularly the HSI products as already reported using the U5 substrate (26).

However, this system did not allow the analysis of the structure of the integration products, *i.e.* viral and genomic DNA sequences found at the integration sites. To better ascertain this point and to address the question of whether integration can take place in an eukaryote cell starting from a 2-LTR junction-containing substrate, we first used the previously characterized yeast integration model (17).

### ***A plasmid encompassing the 2-LTR junction can be integrated in the genome of *Saccharomyces cerevisiae* expressing HIV-1 IN***

The U5•U3 circle was used as substrate for HIV-1 IN-dependent integration in yeast (Fig. 1A). After transformation of the JSC310 Zeocin-sensitive yeast strains expressing HIV-1 IN with this circular putative integration substrate, Zeocin-resistant clones were selected from 2 to 5 h post-transformation (Fig. 4A). Importantly, the processed product of Fig. 1C, *i.e.* the product resulting from cleavage of the plasmid with the palindromic sequence by IN (named U5•U3 processed circle, Fig. 1A), was purified and used as a substrate. As shown in Fig. 4A, both U5•U3 circle and U5•U3 processed circle substrates were able to be integrated into yeast genomic DNA after transformation of IN-expressing cells. Moreover, the U5•U3 processed circle showed a higher integration efficiency suggesting that the limiting step of the process was the DNA cleavage. Comparison of integration efficiency was also performed with the linear U5•U3 substrate, the Random circle substrate, and by using the D116A IN expressed in yeast cells (Fig. 4B). Very few clones were selected in the cases of the Random circle and the D116A IN catalytic mutant, highly suggesting that the integration was mediated by the catalytic activity of IN (Fig. 4B). Even if a higher number of *zeo*<sup>R</sup> clones was obtained using the classical linear substrate highlighting a better integration efficiency with this DNA, the number of *zeo*<sup>R</sup> clones obtained with the palindrome-containing plasmid was significantly higher than in control experiments. To confirm that the *zeo*<sup>R</sup> clones selection was actually due to HIV-1

IN-dependent integration events, the selected clones were further analyzed by sequencing.

### Sequence analyses of the pseudo-viral integrated DNA ends and the cellular integration loci

The integrated products were then further analyzed by sequencing the viral extremities fused to the cellular DNA (Fig. 4, C and D), as reported under “Experimental procedures.” Both viral DNA ends and flanking cellular DNA sequences of pseudo-provirus derived from U5·U3 circles and U5·U3 processed circles substrates were compared with the integrants selected using the linear U5·U3 substrate. As reported in Fig. 4C, similar cellular sequences were found using the linear U5·U3 substrate and the U5·U3 processed circles because, in both cases, about 50% of the integrants displayed the typical 5-bp duplication at both plasmid-genomic DNAs junctions. Interestingly, when the U5·U3 circle was used in the yeast integration experiment, we observed a clear improvement of the reaction fidelity because in that case the percentage of accurate 5-bp duplication was increased from 50 to 80–90% (Fig. 4C). Then, the analysis of the viral DNA ends sequences indicated that when the linear U5·U3 substrate was used, a large percentage of integrants displayed the typical AGCA viral extremity, as expected from the correct 3′-processing step (Fig. 4D). Interestingly, all integrated events displaying this sequence (AGCA) are obtained from events highlighting the 5-bp duplication suggesting a better quality of integration using the palindromic substrate. Some defective ends were also selected, but when the U5·U3 circle substrates (processed or not) were assayed, we observed a higher number of defective viral ends structures in addition to the expected correct structure, indicating a defect in terms of fidelity. Interestingly, the profile observed for the viral DNA ends sequences of integrants from the linear U5·U3 substrate was similar to the one found after *in vitro* cleavage of the U5·U3 DNA substrate by IN alone (Fig. 1B, bottom panel). Moreover, as in the case of *in vitro* cleavage of U5·U3 DNA substrate by IN/LEDGF, the number of blunt viral DNA ends was increased with the circular U5·U3 substrates (processed or not) (Fig. 4D).

### The LTR-LTR junction cleavage leads to correct integration events involving 5-bp duplication of the host cell genome in infected cells

To better ascertain whether integration can take place from the 2-LTR junction in the context of viral infection, we introduced in the genomic sequence of a lentiviral vector (pHR′-CMV-GFP) either a 175-bp palindromic sequence mimicking the canonical LTR-LTR junction (PAL+, 5′-CAGTACTG-3′) or a 175-bp sequence for which the central palindrome has been modified (PAL−, 5′-CACATGTG-3′) between the CMV promoter and the cDNA encoding the eGFP. Among the different integration events (leading to neomycin resistance except for form 3, which is coupled to the formation of form 2), any event that originates from PAL cleavage would lead to GFP negative cells as the CMV promoter will be separated from the eGFP cDNA (Fig. 5A). Note that IN-independent insertion events, could also lead to GFP negative cells (Fig. 5A, form 6). However, our experiments using IN defective (D116N) vectors did not allow the selection of neomycin-resistant cells (data not

shown) highly suggesting that IN-independent integration events were negligible in these conditions.

The two constructions (PAL+ and PAL−) have been used for MT4 cells infection and neomycin was added at d4 post-infection at 1 mg/ml. For the PAL− vectors, 90–95% of the neomycin-resistant cells expressed the GFP due to a standard integration process (Fig. 5A, form 1). For the PAL+ vectors, the part of the neomycin-resistant cells also positive for GFP expression significantly decreased (70–77%) (Fig. 5B). The 20% of the neomycin-resistant cells that did not express GFP could reasonably result from the cleavage of the PAL sequence and a subsequent integration into the host genome. 30 individual neomycin-resistant clones and negative for GFP expression have been isolated. To ensure that the neomycin resistance is actually due to integration using PAL and/or LTR sequences, we first checked that these GFP negative clones did not harbor the PAL sequence. As expected, none of the 30 clones analyzed harbored a complete PAL sequence. We then designed a set of PCR experiments to characterize these clones (Fig. 5A, a to d). The first PCR (a) allowed (i) to detect the presence of Neo cDNA and the 5′ moiety of the PAL sequence and (ii) to detect all integration forms originating from the use of PAL and/or LTR sequences. Among 30 clones, 25 were negative for the PCR “a” and were not further analyzed. The 5 other clones were tested in PCR b (detecting forms 3, 4, and 5), c (detecting forms 2, 4, and 5), and d (detecting forms 4 and 5) (Fig. 5A). As expected, all 5 clones were positive in PCR c, 3 clones were positive in PCR b, and 1 clone was positive in PCR d. The sequences of the insertion sites showed clearly a 5-bp duplication for the 5 clones (Fig. 5C) that is typical of HIV-1 IN-dependent integration. We can note that one clone seems to be due to the integration of 1-LTR circle using PAL sequence as substrate for cleavage and strand transfer (clone 9 corresponding to the form 4). For the other 4 clones, the integration is due to the usage of both PAL and LTR sequences.

Altogether, our results demonstrate that IN can cleave specifically the internal palindromic sequence (at the PAL level) in the viral context, leading to proper integration events. In this setting, efficiency of integration mediated by internal cleavage of the PAL junction is estimated at 17% (5 clones displaying integration from PAL among 30 clones analyzed) but this percentage is probably underestimated because recombination from the PAL sequence with the LTR could occur.

Our results suggest that integration from a 2-LTR substrate could process through a three-step mechanism, a proper two-step mechanism for the LTR-LTR junction cleavage including the blunt cleavage of the palindromic LTR-LTR junction and the subsequent 3′-processing, and finally strand-transfer. Brown and colleagues (27) reported that, in the case of murine leukemia virus, viral intermediates involved in the integration process displayed a 2-mer overhang instead of 4-mer overhang. Therefore, they excluded the roles of the palindromic junction and 2-LTR substrates because they assume that the cleavage of this junction should lead to a 4-mer overhang (a reasonable hypothesis based on a one-step cleavage mechanism) (27). Here, we addressed the possibility that this could be due to a weak sensitivity in the detection because the 2-LTR circles fraction is very weak in a WT infection. We then also characterized

## Integrase and 2-LTR circles

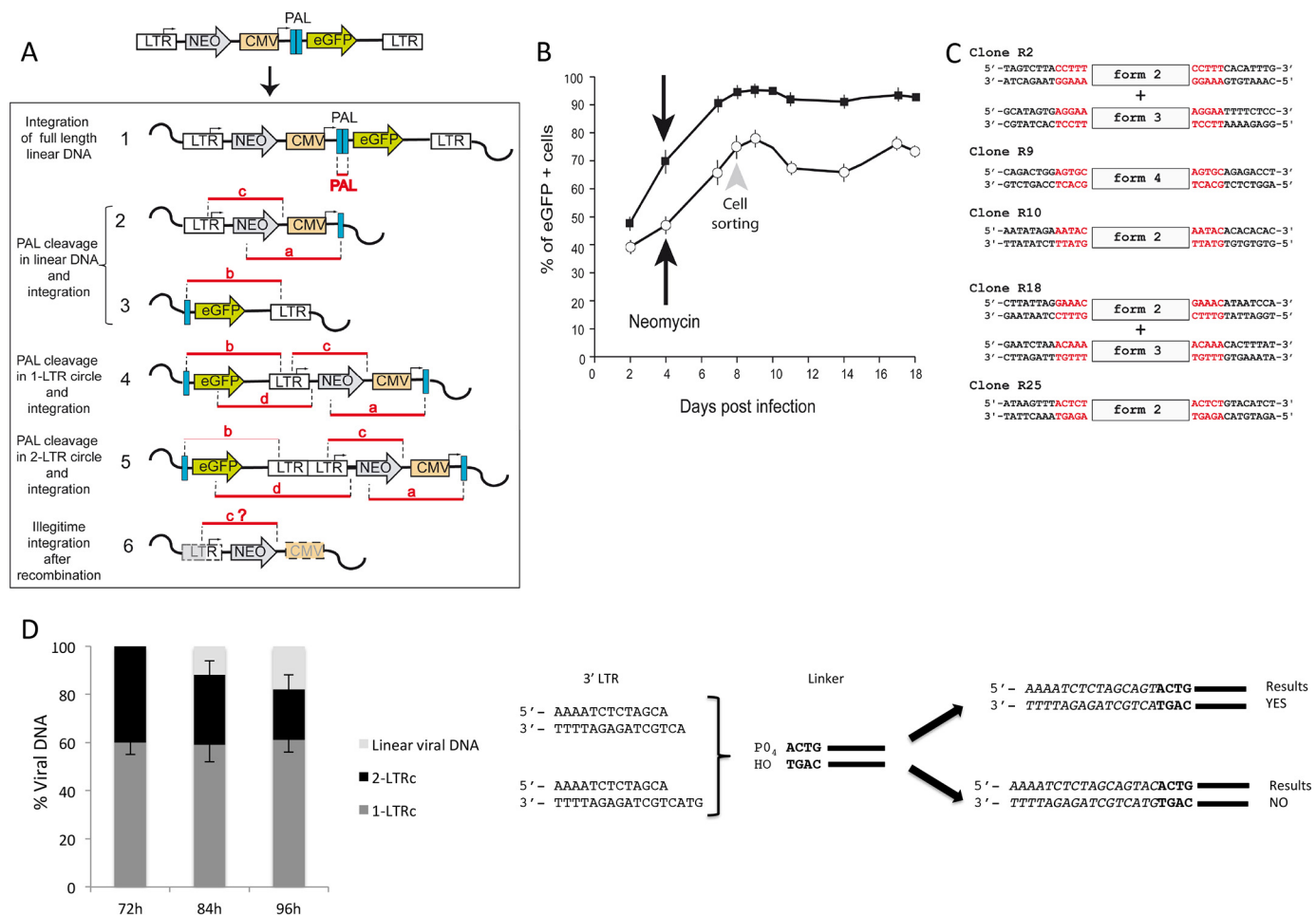


**Figure 5. The palindromic sequence is involved in IN-dependent integration in the virological context.** A shows the PAL sequence construction (175 bp of the U5-U3 sequence) and the possible integration events using only LTR extremities (form 1) or only PAL extremities (forms 4 and 5), or a combination of both (forms 2 and 3). Form 6 represents unwanted integration events possibly due to recombination occurring during reverse transcription. The designed PCR experiments are represented in *red*. B, flow cytometry analysis during PAL+ and PAL- infections. Neomycin was added 4 days post-infection. NeoR/GFP- cells were sorted 8 days post-infection. C, sequences of the integration sites. Results are from three representative independent experiments, mean  $\pm$  S.D. (*error bars*). D, sequences of linear viral DNA after Raltegravir removal. Cells were infected in the same conditions as already described (15). Briefly, MT4 cells were infected with NLENG1-ES-IRES WT pseudotyped with vesicular stomatitis virus-G envelope in the presence of Raltegravir (500 nM). 72 h post-infection, cells were washed and fresh medium, without Raltegravir, was added. 2-LTR circles (2-LTRc, *black column*); 1-LTR circles (1-LTRc, *gray column*), and linear viral DNA (*light gray column*) were quantified by quantitative PCR as already described (15). Linear viral DNA was sequenced by a LM-PCR approach using a blunt ended linker at 84 and 96 h post-infection (4). All sequences displayed the same pattern highlighting the canonical 5'-end of the 3' LTR (5'-CAGT end). In *italic*, the sequence of the viral DNA; in *bold*, the sequence of the linker.

these viral intermediates by an independent approach based on ligation-mediated PCR (LM-PCR) under optimal conditions regarding the number of 2-LTR circles (*i.e.* presence of a well-known anti-integrase drug: Raltegravir, which leads to a strong 2-LTR circles accumulation). To characterize the viral ends originating from the 2-LTR circles, MT4 cells were infected in the presence of 500 nM Raltegravir. Three days post-infection, only 2-LTR and 1-LTR circles were detected by quantitative PCR (Fig. 5D). Importantly, in these conditions, no linear DNA can be detected. When Raltegravir is removed from the cell medium, *de novo* linear DNA can be detected at 84 and 96 h post-infection concomitant to a decrease in 2-LTR circles. These results clearly indicate that *de novo* linear DNA originates from 2-LTR circles confirming our previous report (15). In the present study, the newly formed linear DNA was sequenced (at 84 and 96 h post-infection) by a LM-PCR approach (4) (Fig. 5D). We found that all linear viral DNA harbor a 2-mer overhang with the canonical 5'-CAGT end and not

a 4-mer overhang according to the results found by Brown and colleagues (27). Our results regarding the 2-mer overhang are in accordance with those described in Fig. 1D showing that cleavage of the palindromic DNA substrate by IN is compatible with the formation of blunt-ended DNA product. Altogether, our results reconcile the apparent discrepancy concerning the role of the palindromic junction in the integration process, suggesting that cleavage of the palindromic sequence occurs by a two-steps mechanism: the formation of the blunt product followed by a standard 3'-processing reaction leading to the canonical 2-mer overhang.

Taken together our data show that circular DNA containing a 2-LTR junction can be integrated into chromosomes in both a yeast and infected cells context. Biochemical experiments indicated that the 2-LTR junction can be cleaved and subsequently integrated in a concerted manner by HIV-1 IN *in vitro*. It is important to note that 2-LTR circles only represent a small fraction of viral genomes in infected cells with a WT virus (28).

Therefore, during a WT infection, when linear DNA is abundant, such a linear DNA directly issued from reverse transcription corresponds to the main substrate for integration. Our results highly suggest that a circular form of DNA containing the palindromic LTR-LTR junction can serve as an alternative substrate for integration and that this role is enhanced in conditions where 2-LTR circles have been pre-accumulated representing nearly half of the viral genome, for example, using strand-transfer inhibitors such as Raltegravir (15). In conditions where the IN inhibitor is destabilized from the pre-integration complex, the palindromic junction can be cleaved leading to *de novo* linear viral DNA that can be further integrated in the host cell genome.

Taking into account that (i) in average 50% of the LTR-LTR junction display canonical palindromic features studied in this report (from 20 to 76% depending of the study (29, 30)), (ii) the efficiency of LTR-LTR cleavage is about 50%, and (iii) 50% of the resulting linear DNA is integrated, we estimate that ~10% of the 2-LTR circles can be used as a substrate for viral DNA integration. This leads to a new interpretation for the putative function of the 2-LTR circles found in HIV-1-infected cells. Indeed, our data highly suggest that these structures can be integrated in further integration steps and, thus, could serve as stock for multiple integration events.

## Experimental procedures

### Proteins

HIV-1 IN was purified using previously described protocols with some modification (20). HIV-1 IN was expressed in *Escherichia coli* (Rosetta) and the cells were lysed in buffer containing 50 mM Hepes, pH 7.5, 5 mM EDTA, 1 mM DTT, 1 mM PMSF. The lysate was centrifuged and IN extracted from the pellet in buffer containing 1 M NaCl, 50 mM Hepes, pH 7.5, 1 mM EDTA, 1 mM DTT, 7 mM CHAPS. The protein was then purified on a butyl column equilibrated with 50 mM Hepes, pH 7.5, 200 mM NaCl, 1 M ammonium sulfate, 100 mM EDTA, 1 mM DTT, 7 mM CHAPS, 10% glycerol. The protein was further purified on a heparin column equilibrated with 50 mM Hepes, pH 7.5, 200 mM NaCl, 100 mM EDTA, 1 mM DTT, 7 mM CHAPS, glycerol (10%).

LEDGF was expressed in PC2 bacteria and the cells were lysed in lysis buffer containing 20 mM Tris, pH 7.5, 1 M NaCl, 1 mM PMSF, and added lysozyme and protease inhibitors. The protein was purified by nickel-affinity chromatography and the His tag was removed with 3C protease at 4 °C overnight. After dilution down to 150 mM NaCl, the protein was further purified on an SP column equilibrated with 25 mM Tris, pH 7.5, 150 mM NaCl (gradient from 150 mM to 1 M NaCl), then a final 2 mM DDT was added and concentrated for gel filtration. Gel filtration was performed on a Superdex 200 column (GE Healthcare) equilibrated with 25 mM Tris, pH 7.5, 500 mM NaCl. 2 mM DTT was added to the eluted protein. The protein was then concentrated to about 10 mg/ml. The IN-LEDGF/p75 complex was reconstituted to a IN/LEDGF ratio of 2. A SDS-PAGE gel stained with Coomassie was provided (Fig. 1B) and show a purity >95% for each protein.

### *In vitro* concerted integration

Standard concerted integration reactions were performed mainly as described previously (20) using purified HIV-1 IN (0.25 to 3  $\mu$ M), circular target DNA plasmids pBSK-zeo (100 ng), and the different 38-bp double-stranded 5'-end-labeled donor DNA (10 ng) (described in Fig. 1A) and mimicking the 2-LTR junction (U5·U3), the LTR viral end (U5), or displaying a randomized nonviral sequence (Random). ODN used to form the U5·U3 DNA were: U5, 5'-TGTGGAAAATCTCTAGCAGTACTGGAAGGGCTAATTTG and U3, 5'-CAAATTAGCCCTTCCAGTACTGCTAGAGATTTTCCACA. IN was incubated for 20 min at 4 °C with both the donor and the acceptor DNA before adding the reaction mixture (20 mM Hepes, pH 7.5, 10 mM DTT, 10 mM MgCl<sub>2</sub>, 15% DMSO, 8% PEG, 30 mM NaCl) in a final volume of 10  $\mu$ l. The reaction was further incubated for 90 min at 37 °C, and was then stopped by adding a phenol/isoamyl alcohol/chloroform mix (24/1/25, v/v/v). The aqueous phase was loaded on a vertical 1% agarose gel in the presence of 1% bromphenol blue and 1 mM EDTA. After separation of the products, the gel was treated with 5% TCA for 20 min, dried, and autoradiographed. After reaction, three types of products are detected: donor/donor products (d/d) corresponding to the strand transfer of one viral end from one donor molecule to another one, circular half-site (HSI) products corresponding to the strand transfer of one viral end from one donor molecule to a circular acceptor plasmid, and linear full-site (FSI) products corresponding to the strand transfer of two viral ends from two independent donor molecules into a circular acceptor plasmid leading to its linearization.

### DNA endonuclease assay

Standard reactions were performed as described previously (31). The pGEM-T-2LTR (U5·U3 circle) or the pGEM-T-Random (Random circle) described in Fig. 1A were used as DNA substrate. Purified IN (0.5–1  $\mu$ M) was incubated with 300 ng of plasmid DNA in a reaction mixture of 10  $\mu$ l containing 20 mM Hepes, pH 7.5, 10 mM DTT, 0.05% Nonidet P-40, 30 mM NaCl and MnCl<sub>2</sub> or MgCl<sub>2</sub> (7.5 mM). The reaction mixture was incubated for 1 h at 37 °C and stopped by addition of 2  $\mu$ l of 1% bromphenol blue and 1 mM EDTA (standard conditions). Samples were analyzed on a 1% agarose minigel containing ethidium bromide. Electrophoresis was carried out and DNA was detected by fluorescence upon exposure to UV light. Activity was evaluated by quantification of the bands corresponding to the different topological forms of the plasmid using ImageJ software after scanning.

### *In vivo* yeast integration assay

Yeast integration assays were performed essentially as described in Ref. 17. JSC310 yeast cells harboring either pHIV1SF2IN or pHIV1SF2IN-D116A vectors were grown for 72 h under maximal expression conditions (10 ml of yeast nitrogen base containing 0.1% glucose and supplemented with the required amino acids) until an OD<sub>600 nm</sub> of about 10 was reached (stationary phase). Yeast aliquots were used for transformation with an excess of the DNA substrate under conditions previously described (32). After transformation, 10<sup>9</sup> viable cells, calculated by counting the number of cells recovered after

## Integrase and 2-LTR circles

plating on nonselective medium, were cultured in YCAD liquid medium for 1–5 h and then plated on solid YCAD medium supplemented with Zeocin (400 µg/ml) to select the cells expressing the *Sh ble* gene from the DNA substrate. After 5 days of culture, resistant clones were recovered, stocked, and further analyzed. Transformants were selected on medium lacking uracil and histidine.

### Sequence analysis of the plasmid cleavage events

Sequencing was performed according to the LM-PCR method, using the 11GTb linker (ODN, 5'-GTGAATTCAGATC-3', hybridized with ODN, 5'-GCGGTGACCCGGGAGATCTGAATTC-3'), as previously described by Munir and colleagues (33). Briefly, a ligation reaction mixture was carried out by addition of 11GTb linker (30 nM) to plasmid cleavage products in the presence of 10 units of ligase from the Quick ligation kit (New England Biolabs) according to the manufacturer's instructions (2 h, room temperature, 20 µl of final volume), and submitted to PCR. After amplification of the ligation product and purification on an agarose gel, DNA fragments were sequenced.

### Sequence analysis of the integration events

Sequencing was performed using chromosomal DNA digested by BamHI, religated with T4 DNA ligase (Promega), and amplified using 5'-U3-junction (5'-GATGCGCGGAGTCGA-3') and 3'-U5-junction (5'-AGACGCGTGTACGCATGTA-3') primers. The amplification products were used in PCR-based sequencing (ABI Prism big dye terminator cycle sequencing ready reaction kit, Applied Biosystems) using the same primers.

### Cells and viruses

HIV-1 stocks were prepared by transfecting 293T cells with the various HIV-1 molecular clones derived from HpGK and the vesicular stomatitis virus-G plasmid. The viral construction encompasses the CMV promoter with eGFP and the 175-bp LTR-LTR junction (PAL+). A second construction was obtained by disrupting the palindromic sequence (PAL-). MT4 cells were infected with 60 ng of p24<sup>gag</sup> antigen per 10<sup>6</sup> cells, corresponding to a multiplicity of infection of 0.3. Cells were analyzed during the experiment and neomycin-resistant GFP- cells were sorted at 8 days post-infection using a FACS Aria SORP (Institut Gustave Roussy platform).

### Integration sites analysis

After cells sorting, cells were grown and DNA was extracted using a QiaAmp blood kit (Qiagen). Integration sites were determined using MfeI restriction enzyme and LM-PCR as previously described (34). The primers sets for analysis were (Fig. 5A): PCR PAL, PAL forward (5'-GACACCGACTCTAGCTAGAG-3') and PAL reverse (5'-CACCATGAATTCCTCGAGT-3'); PCR a, NEO129 (5'-ACAA-CAGACAATCGGCTGCT-3') and AA55M (5'-GCTAGAGATTTTCCACTGACTAA-3'); PCR b, HIVR1 (5'-ACTGGTACTAGCTTGTAGCACCATCCA-3') and rev-PALsal1 (5'-CAAGGCTACTTCCCTGGTTCGAC-3'); PCR c, MH531 (5'-TGTGTGCCCGTCTGTTGTGT-3') and

NEO130 (5'-TCGTCCAGATCATCCTGATC-3'); and PCR d, GFPfor (5'-ACCACTACCAGCAGAACACC-3') and PHR'-LTRfor (5'-CCCTTTCGCTTCAAGTCCC-3').

---

*Author contributions*—C. R., S. T., E. T., P. L., H. L., V. P., and O. D. conceptualization; C. R., S. T., E. T., P. L., S. M., F. S., V. P., and O. D. formal analysis; C. R., S. T., E. T., D. L., and O. D. methodology; D. L. data curation; E. D., V. P., and O. D. writing-original draft; O. D. supervision; O. D. funding acquisition.

---

*Acknowledgment*—We thank Yann Lecluse (Institut Gustave Roussy platform) for technical assistance concerning cell sorting.

---

### References

1. Delelis, O., Carayon, K., Saïb, A., Deprez, E., and Mouscadet, J. F. (2008) Integrase and integration: biochemical activities of HIV-1 integrase. *Retrovirology* **5**, 114 [CrossRef Medline](#)
2. Engelman, A., Mizuuchi, K., and Craigie, R. (1991) HIV-1 DNA integration: mechanism of viral DNA cleavage and DNA strand transfer. *Cell* **67**, 1211–1221 [CrossRef Medline](#)
3. Sinha, S., and Grandgenett, D. P. (2005) Recombinant human immunodeficiency virus type 1 integrase exhibits a capacity for full-site integration *in vitro* that is c that of purified preintegration complexes from virus-infected cells. *J. Virol.* **79**, 8208–8216 [CrossRef Medline](#)
4. Munir, S., Thierry, S., Subra, F., Deprez, E., and Delelis, O. (2013) Quantitative analysis of the time-course of viral DNA forms during the HIV-1 life cycle. *Retrovirology* **10**, 87 [CrossRef Medline](#)
5. Fischer, M., Trkola, A., Joos, B., Hafner, R., Joller, H., Muesing, M. A., Kaufman, D. R., Berli, E., Hirschel, B., Weber, R., Günthard, H. F., and Swiss HIV-1 Cohort Study (2003) Shifts in cell-associated HIV-1 RNA but not in episomal HIV-1 DNA correlate with new cycles of HIV-1 infection *in vivo*. *Antivir. Ther.* **8**, 97–104 [Medline](#)
6. Wu, Y. T., and Marsh, J. W. (2003) Early transcription from nonintegrated DNA in human immunodeficiency virus infection. *J. Virol.* **77**, 10376–10382 [CrossRef Medline](#)
7. Yoder, K., Sarasin, A., Kraemer, K., McIlhatton, M., Bushman, F., and Fishel, R. (2006) The DNA repair genes XPB and XPD defend cells from retroviral infection. *Proc. Natl. Acad. Sci. U.S.A.* **103**, 4622–4627 [CrossRef Medline](#)
8. Kilzer, J. M., Stracker, T., Beitzel, B., Meek, K., Weitzman, M., and Bushman, F. D. (2003) Roles of host cell factors in circularization of retroviral DNA. *Virology* **314**, 460–467 [CrossRef Medline](#)
9. Hazuda, D. J., Felock, P., Witmer, M., Wolfe, A., Stillmock, K., Grobler, J. A., Espeseth, A., Gabryelski, L., Schleif, W., Blau, C., and Miller, M. D. (2000) Inhibitors of strand transfer that prevent integration and inhibit HIV-1 replication in cells. *Science* **287**, 646–650 [CrossRef Medline](#)
10. Reigadas, S., Andréola, M. L., Wittkop, L., Cosnefroy, O., Anies, G., Recordon-Pinson, P., Thiebaut, R., Masquelier, B., and Fleury, H. (2010) Evolution of 2-long terminal repeat (2-LTR) episomal HIV-1 DNA in raltegravir-treated patients and in *in vitro* infected cells. *J. Antimicrob. Chemother.* **65**, 434–437 [CrossRef Medline](#)
11. Sloan, R. D., and Wainberg, M. A. (2011) The role of unintegrated DNA in HIV infection. *Retrovirology* **8**, 52 [CrossRef Medline](#)
12. Chan, C. N., Trinité, B., Lee, C. S., Mahajan, S., Anand, A., Wodarz, D., Sabbaj, S., Bansal, A., Goepfert, P. A., and Levy, D. N. (2016) HIV-1 latency and virus production from unintegrated genomes following direct infection of resting CD4 T cells. *Retrovirology* **13**, 1 [CrossRef Medline](#)
13. Delelis, O., Parissi, V., Leh, H., Mbemba, G., Petit, C., Sonigo, P., Deprez, E., and Mouscadet, J. F. (2007) Efficient and specific internal cleavage of a retroviral palindromic DNA sequence by tetrameric HIV-1 integrase. *PLoS One* **2**, e608 [CrossRef Medline](#)
14. Delelis, O., Petit, C., Leh, H., Mbemba, G., Mouscadet, J. F., and Sonigo, P. (2005) A novel function for spumaretrovirus integrase: an early requirement for integrase-mediated cleavage of 2 LTR circles. *Retrovirology* **2**, 31 [CrossRef Medline](#)

15. Thierry, S., Munir, S., Thierry, E., Subra, F., Leh, H., Zamborlini, A., Saenz, D., Levy, D. N., Lesbats, P., Saïb, A., Parissi, V., Poeschla, E., Deprez, E., and Delelis, O. (2015) Integrase inhibitor reversal dynamics indicate unintegrated HIV-1 DNA initiate *de novo* integration. *Retrovirology* **12**, 24 [CrossRef Medline](#)
16. Zhang, D. W., He, H. Q., and Guo, S. X. (2014) Hairpin DNA probe-based fluorescence assay for detecting palindrome cleavage activity of HIV-1 integrase. *Anal. Biochem.* **460**, 36–38 [CrossRef Medline](#)
17. Desfarges, S., San Filippo, J., Fournier, M., Calmels, C., Caumont-Sarcos, A., Litvak, S., Sung, P., and Parissi, V. (2006) Chromosomal integration of LTR-flanked DNA in yeast expressing HIV-1 integrase: down regulation by RAD51. *Nucleic Acids Res.* **34**, 6215–6224 [CrossRef Medline](#)
18. Cherepanov, P., Maertens, G., Proost, P., Devreese, B., Van Beeumen, J., Engelborghs, Y., De Clercq, E., and Debysers, Z. (2003) HIV-1 integrase forms stable tetramers and associates with LEDGF/p75 protein in human cells. *J. Biol. Chem.* **278**, 372–381 [CrossRef Medline](#)
19. Reigadas, S., Anies, G., Masquelier, B., Calmels, C., Stuyver, L. J., Parissi, V., Fleury, H., and Andreola, M. L. (2010) The HIV-1 integrase mutations Y143C/R are an alternative pathway for resistance to raltegravir and impact the enzyme functions. *PLoS One* **5**, e10311 [CrossRef Medline](#)
20. Lesbats, P., Métiot, M., Calmels, C., Baranova, S., Nevinsky, G., Andreola, M. L., and Parissi, V. (2008) *In vitro* initial attachment of HIV-1 integrase to viral ends: control of the DNA specific interaction by the oligomerization state. *Nucleic Acids Res.* **36**, 7043–7058 [CrossRef Medline](#)
21. Hazuda, D., Iwamoto, M., and Wenning, L. (2009) Emerging pharmacology: inhibitors of human immunodeficiency virus integration. *Annu. Rev. Pharmacol.* **49**, 377–394 [CrossRef](#)
22. Faure, A., Calmels, C., Desjobert, C., Castroviejo, M., Caumont-Sarcos, A., Tarrago-Litvak, L., Litvak, S., and Parissi, V. (2005) HIV-1 integrase cross-linked oligomers are active *in vitro*. *Nucleic Acids Res.* **33**, 977–986 [CrossRef Medline](#)
23. Krishnan, L., Li, X., Naraharisetty, H. L., Hare, S., Cherepanov, P., and Engelman, A. (2010) Structure-based modeling of the functional HIV-1 intasome and its inhibition. *Proc. Natl. Acad. Sci. U.S.A.* **107**, 15910–15915 [CrossRef Medline](#)
24. Li, M., and Craigie, R. (2009) Nucleoprotein complex intermediates in HIV-1 integration. *Methods* **47**, 237–242 [CrossRef Medline](#)
25. Li, M., Mizuuchi, M., Burke, T. R., Jr., and Craigie, R. (2006) Retroviral DNA integration: reaction pathway and critical intermediates. *EMBO J.* **25**, 1295–1304 [CrossRef Medline](#)
26. Maillot, B., Lévy, N., Eiler, S., Crucifix, C., Granger, F., Richert, L., Didier, P., Godet, J., Pradeau-Aubretton, K., Emiliani, S., Nazabal, A., Lesbats, P., Parissi, V., Mely, Y., Moras, D., Schultz, P., and Ruff, M. (2013) Structural and functional role of IN1 and LEDGF in the HIV-1 preintegration complex. *PLoS One* **8**, e60734 [CrossRef Medline](#)
27. Brown, P. O., Bowerman, B., Varmus, H. E., and Bishop, J. M. (1989) Retroviral integration: structure of the initial covalent product and its precursor, and a role for the viral IN protein. *Proc. Natl. Acad. Sci. U.S.A.* **86**, 2525–2529 [CrossRef Medline](#)
28. Butler, S. L., Hansen, M. S., and Bushman, F. D. (2001) A quantitative assay for HIV DNA integration *in vivo*. *Nat. Med.* **7**, 631–634 [CrossRef Medline](#)
29. Bona, R., Baroncelli, S., D'Etto, G., Andreotti, M., Ceccarelli, G., Filati, P., Leone, P., Blasi, M., Michelini, Z., Galluzzo, C. M., Mallano, A., Vullo, V., and Cara, A. (2013) Effects of raltegravir on 2-long terminal repeat circle junctions in HIV type 1 viremic and aviremic patients. *AIDS Res. Hum. Retroviruses* **29**, 1365–1369 [CrossRef Medline](#)
30. Svarovskaia, E. S., Barr, R., Zhang, X., Pais, G. C., Marchand, C., Pommier, Y., Burke, T. R., Jr., and Pathak, V. K. (2004) Azido-containing diketo acid derivatives inhibit human immunodeficiency virus type 1 integrase *in vivo* and influence the frequency of deletions at two-long-terminal-repeat-circle junctions. *J. Virol.* **78**, 3210–3222 [CrossRef Medline](#)
31. Parissi, V., Caumont, A., de Soultrait, V. R., Desjobert, C., Calmels, C., Fournier, M., Gourgue, G., Bonneu, M., Tarrago-Litvak, L., and Litvak, S. (2003) The lethal phenotype observed after HIV-1 integrase expression in yeast cells is related to DNA repair and recombination events. *Gene* **322**, 157–168 [CrossRef Medline](#)
32. Chen, J. W., Evans, B. R., Yang, S. H., Araki, H., Oshima, Y., and Jayaram, M. (1992) Functional-analysis of box-I mutations in yeast site-specific recombinase-Flp and recombinase-R: pairwise complementation with recombinase variants lacking the active-site tyrosine. *Mol. Cell. Biol.* **12**, 3757–3765 [CrossRef Medline](#)
33. Munir, S., Thierry, E., Malet, I., Subra, F., Calvez, V., Marcelin, A. G., Deprez, E., and Delelis, O. (2015) G118R and F121Y mutations identified in patients failing raltegravir treatment confer dolutegravir resistance. *J. Antimicrob. Chemother.* **70**, 739–749 [Medline](#)
34. Wu, X., Li, Y., Crise, B., and Burgess, S. M. (2003) Transcription start regions in the human genome are favored targets for MLV integration. *Science* **300**, 1749–1751 [CrossRef Medline](#)